Article

Not peer-reviewed version

Hemocompatibility of Membrane Lung Components from Extracorporeal Membrane Oxygenation with Different Antithrombogenic Coatings

Christopher Thaus , Elena Hofrichter , Matthias Lubnow , Lars Krenkel , Karla Lehle *

Posted Date: 6 December 2024

doi: 10.20944/preprints202412.0615.v1

Keywords: ECMO; platelet activation; platelet adhesion; hemolysis; hemocompatibility

 doi:10.20944/preprints202412.0615.v1

Article

Hemocompatibility of Membrane Lung Components from Extracorporeal Membrane Oxygenation with Different Antithrombogenic Coatings

Christopher Thaus [1], Elena Hofrichter [1], Matthias Lubnow [2], Lars Krenkel [3] and Karla Lehle [1,*]

[1] Department of Cardiothoracic Surgery, University Hospital Regensburg, Regensburg, Germany
[2] Department of Internal Medicine II, University Hospital Regensburg, Regensburg, Germany
[3] Regensburg Center of Biomedical Engineering, Ostbayerische Technische Hochschule, Regensburg, Germany
* Correspondence: karla.lehle@ukr.de; Tel.: 0049 941 944 9901

Abstract: Thrombus formation within extracorporeal membrane oxygenation (ECMO) devices remained a critical complication. One reason seems to be the contact of blood with large artificial surfaces within the membrane lung (ML). The aim was to test the hemocompatibility of different naïve ECMO materials. Blood and platelets from five healthy volunteers were incubated with gas exchange (GF) and heat exchange fibers (HE) from four different commercial available new MLs representing different antithrombogenic coatings. Adherent platelets were stained with rhodamine-phalloidin. Surface coverage was quantified with ImageJ. Non-adherent platelets were stained with antibodies (CD6²P, PAC-1, CD61) and fibrinogen to detect platelet activation with flow cytometry. Hemolysis of red blood cells after material contact was detected. All ECMO-materials were non-hemolytic and did not induce platelet activation. However, platetelet adhesion (median (IQR)) was significantly elevated on uncoated GFs made of polymethylpentene (GF-PMP; 12 (7-19)%) and on GFs from the Hilite-MLs (GF-Hilite; 13 ((8-19)%) compared to the other materials. In vitro testing of platelet adhesion disclosed significant differences of ECMO-materials with different antithrombogenic surface coatings. Instead, circulating platelets remained non-activated. ECMO-materials and its coatings were non-hemolytic. Finally, this study confirmed the good hemocompatibility of GFs and HEs from commerciall available MLs.

Keywords: ECMO; platelet activation; platelet adhesion; hemolysis; hemocompatibility

1. Introduction

Venovenous extracorporeal membrane oxygenation (VV ECMO) is used in critical care to manage patients with severe respiratory failure [1]. ECMO brings patient blood into contact with artificial surfaces from the circuit under non-physiologial flow conditions which can cause thrombosis and bleeding [2,3]. In particular, the membrane lung (ML) - a critical component of the ECMO circuit - is prone to significant thrombus formation due to its large surface area and areas of low, turbulent, and stagnant flow. The incidence of thrombosis within the ECMO circuit ranged between 3 and 22% [4,5]. Despite antithrombogenic surface coatings such as heparin, albumin, phosphorylcholine, or polyethylene oxide (PEO) thrombus formation remained a high risk problem within the ML especially for long-term usage [6-8]. However, detailed standard hemocompatibility assessment of the commercial available coatings are usually only rudimentary due to manufacturer secrets [9,10].

The aim was to test the hemocompatibility of gas exchange fibers (GF) and heat exchange fibers (HE) from different commercial available new ECMO systems with a special focus on the response of platelets on corresponding antithrombogenic surface coatings. The ECMO material was prepared from respective non-used MLs. GFs and HEs from all MLs were incubated with blood/isolated platelets from 5 healthy blood donors and analysed for platelet adhesion, activation and hemolysis.

 doi:10.20944/preprints202412.0615.v1

2. Materials and Methods

2.1. Preparation of Test Material

Test material (GF, gas exchange, and HE, heat exchange fiber mats) was prepared from non-used naïve MLs from four different producers (PLS, Getinge, Rastatt; Hilite 7000LT, Fresenius Medical Care, Bad Homburg; Nautilus, Medtronic, Meerbusch; EOS, LivaNova, Munich, Germany). All GFs consisted of polymethylpentne (PMP), while HEs were made of different materials (Table S1). Each ML was coated with individual antithrombotic coatings (Table S1). Uncoated GFs (GF-PMP, reference material) were kindly provided by Getinge. A band saw was used to remove the housing of the MLs. Sawing particles were withdrawn by suction. The internal block consisting of stacked or wrapped mats of gas exchange and heat exchange membranes was handeld under steril conditions. The outer twenty mats were discarded. Subsequent mats were trimmed with a steril scalpell for hemolysis (1 cm x 2 cm) and platelet adhesion/activation (2 cm x 2 cm) assays ("samples") and stored until usage at room temperature (RT). The samples were identified with GF or HE and respective ML (GF-PLS, GF-Hilite, GF-EOS, GF-Nautilus, HE-PLS, HE-Hilite, HE-Nautilus). Before analysis, test material was soaked in 70% ethanol (30 min), and immerced extensively in sterile physiologic saline (37°C, 30 min).

2.2. Ethics Statement

Prior to blood procurement, the written consent form was given to the healthy volunteers. They read the benefits and risks of participation before expressing his/her willingness by signing the form. All protocols of blood procurement and consent procedure were approved by the Ethics Committee from the University of Regensburg (vote No. 16-101-0322).

2.3. Blood Collection and Preparation of Platelet Rich Plasma

Whole blood was extracted via venipuncture from aspirin-free healthy adult human donors (n=5) and it is prevented from coagulation with ethylenediamine tetraacetic acid (EDTA, 1.2 mg/mL; 6 mL) or trisodium citrate at a volumetric ratio of 9:1 (30 mL).

For the hemolysis assay, EDTA-anticoagulated blood was diluted with physiologic saline (0.9% w/v; NaCl) at a ratio of 1:1.25. For the platelet adhesion/activation assays, citrated blood was stabilized for 30 min at RT with a slight rolling movement. Afterwards, blood samples were centrifuged (300xg, 10 min, RT). The supernatant (= platelet rich plasma, PRP; 1.1 mL) was transferred into another sterile tube. The remaining blood sample was again centrifuged (3x 3,320xg, each 10 min, RT). The supernatant was platelet poor plasma (PPP) that was used to dilute PRP (10% PRP final). All test materials were incubated with blood (hemolysis) and diluted PRP from each blood donor.

2.4. Hemolysis Assay

Test material was incubated with 800 µL aliquots of diluted EDTA-blood (37 °C, 1 h). Nonlysed (NL) and completely lysed (CL) cells were provided by mixing blood with NaCl and distilled water (4:5), respectively. After incubation, the solution of each well was collected and centrifuged (1,200xg, 10 min). The amount of free hemoglobin released from lysed red blood cells (RBC) was quantified by spectrophotometry at 540 nm. The degree of hemolysis (%) can be expressed according to the following formula:

hemolysis rate (%) = $[(OD_{sample}-OD_{NL}) / (OD_{CL}-OD_{NL})] \times 100$

where OD_{sample} is the average absorbance of the test material samples, OD_{NL} is the absorbance of non-lysed cell and OD_{CL} is the absorbance of completely lysed cells [11].

 doi:10.20944/preprints202412.0615.v1

2.5. Platelet Adhesion Assay

After incubation in physiologic saline, test material was transferred to 6-well plates, weighed down with a sterile stainless steel frame and incubated with 1.5 mL diluted PRP in an incubator (60 min, 37°C, 5% CO_2). The supernatant was carefully removed for subsequent flow cytometry (see 2.6). The test material was rinsed carefully in phospate-buffered saline (PBS, pH 7.4) supplemented with bovine serum albumin (BSA, 0.5%) and fixed in paraformaldehyde (final, 1% in PBS) (30 min, RT). Adherent platelets were stained with rhodamine-labeled phalloidin (Invitrogen, Carlsbad, CA, USA) (1:200 diluted in PBS) for the F-actin cytoskeleton (60 min, RT, darkness). Test material was embedded between two coverslips (24 mm x 60 mm) in Fluoromount-G (Southern Biotech, Birmingham, AL, USA) (over night, darkness).

For quantification of adherent platelets (Figure S1), images were captured by a 40x objective using a fluorescence microscope (BZ-8100E Keyence, Neu-Isenburg, Germany) with an integrated camera system. To estimate the extent of cellular deposits, two consecutive capillaries of the stained sample were selected and digitalized. Images from 5 different fields were imported into the ImageJ program (National Institute of Health). Conversion to grayscale was performed to distinguish between areas of aggregates and background. Region of interests (ROI) were selected along two GF fibers (total area of ROI, 1.53 mm^2) and one HE fibers (total area of ROI, 0.77 mm^2). The ROI area was calculated using the scale bar on the images. The area of stained platelets (subdivided into particles with different areas, <10 μm^2, 10-100 μm^2, >100 μm^2) was calculated. The amount of delimitable particles, the particle areas as well as the sum of the area of all particles within the individual ROIs were determined. Total cell density as well as the proportion of different particle sizes relative to the total particle count was calculated.

2.6. Material-Induced Platelet Activation

The supernatant of the platelet adhesion experiments were used to analyze the levels of material-induced platelet activation using a PRP flow cytometry assay. Treatment of PRPs with ADP (50 µM) and PBS (4 min, RT) were used as stimulated and non-stimulated controls, respectively. Detalis on used antibodies and fibrinogen-AlexaFluor488 see supplementary material.

One aliquot of the supernatants and the controls (100 µL) were incubated with the antibodies (PAC-1-FITC, CD62P-PE) (45 min, RT, darkness), fixed with equal volumes of paraformaldehyde (2%, 30 min, RT), washed with PBS/0.5% BSA (2 mL), and centrifuged (520xg, 10 min, RT). Another aliquot (100 µL) was incubated with fibrinogen-AlexaFluor488 (4 min, RT, darkness), fixed with paraformaldehyde, washed, and centrifuged. Cell pellet was resuspended in 100 µL PBS/0.5%BS and stained with the anti-human CD61 antibody (45 min, RT, darkness). Subsequently, cells were washed and centrifuged. Each pellet was resuspended in 500 µL PBS/0.5% BSA, measured by a flow cytometer (FACSCalibur, BD Bioscience) and analyzed with the FlowJo data analysis package (University of Washington, Washington, USA). Platelets stained with PAC-1 and CD62P were identified according to their forward (FSC) and light scatter signal (SSC). These cells were divided into PAC-1-positive and/or CD62P-positive (or both) platelet populations. The proportion of positive cells as well as its median fluorescence intensity (median FI) was analysed. Fibrinogen-stained platelets were identified by CD61-positive fluorescence and 90 degrees SSC. This population was subdivided into non-stimulated (fibrinogen-negative) or stimulated platelets (fibrinogen-positive).

2.7. Statitics

Statistical analysis was done using SigmaStat 3.5 (SYSTAT Software, San Jose, CA, USA). Continuous variables were shown as median (interquartile range, IQR), categorical variables were expressed as frequencies (percentage). Two-way analysis of variance (ANOVA) was used to compare material-induced responses. If there was a statistical significant difference, the parameters at indicated time points were compared using one-way ANOVA. A p-value < 0.05 was considered the threshold of statistical significance.

 doi:10.20944/preprints202412.0615.v1

3. Results

3.1. ECMO Material from Different MLs Was Non-Hemolytic

The surface of engineered scaffolds for blood contact could damage erythrocytes, thereby leading to the release of hemoglobin [12]. The highest degree of hemolysis was provoked by water (completely lysed), where the absorbance of released hemoglobin reached the value of 2.3 ± 0.4 (mean ± standard deviation). In non-lysed cells no hemolysis was observed (0.05 ± 0.01). Contact of blood with test samples resulted in free hemoglobin levels of 0.14 ± 0.01 with no differences comparing the ECMO materials (p=0.977). The degree of hemolysis of blood contacting ECMO materials must be <5% according to ISO 10993-4:2017 standard and ASTM F756-00(2000) [13,14]. As shown in Table 1, the mean hemolysis rate of each ECMO material was below 5% and therefore, all test materials were classified as non-hemolytic.

Table 1. Hemolysis rate of ECMO materials

ECMO material	Hemolysis rate (%)
GF-PMP	4.0 ± 3.0
GF-PLS	3.5 ± 2.5
GF-Hilite	4.3 ± 3.8
GF-EOS	4.1 ± 3.8
GF-Nautilus	4.4 ± 3.8
HE-PLS	3.1 ± 2.9
HE-Hilite	4.2 ± 3.5
HE-Nautilus	3.5 ± 3.8

GF, HE, gas fibers and heat exchangers from respective membrane lungs. Each material was incubated with blood from 5 different healthy blood donors. Data are mean and standard deviation.

3.2. ECMO Material from Different MLs Did Not Induce Platelet Activation

The supernatant of platelet adhesion experiments stands for circulating platelets in contact with ECMO materials. Figure S2 shows a representative FACS analysis of material-induced platelel activation. None of the analyzed ECMO material surfaces induced platelet activation. There was no increase in the frequency of CD62P-positive cells and PAC-1-positive cells (Figure 1A, C). The median fluorescence intensity of respective cell populations remained unchanged (Figure 1B, D). Furthermore, contact of platelets with ECMO material did not increase fibrinogen-binding and CD61 expression (Figure 2).

 doi:10.20944/preprints202412.0615.v1

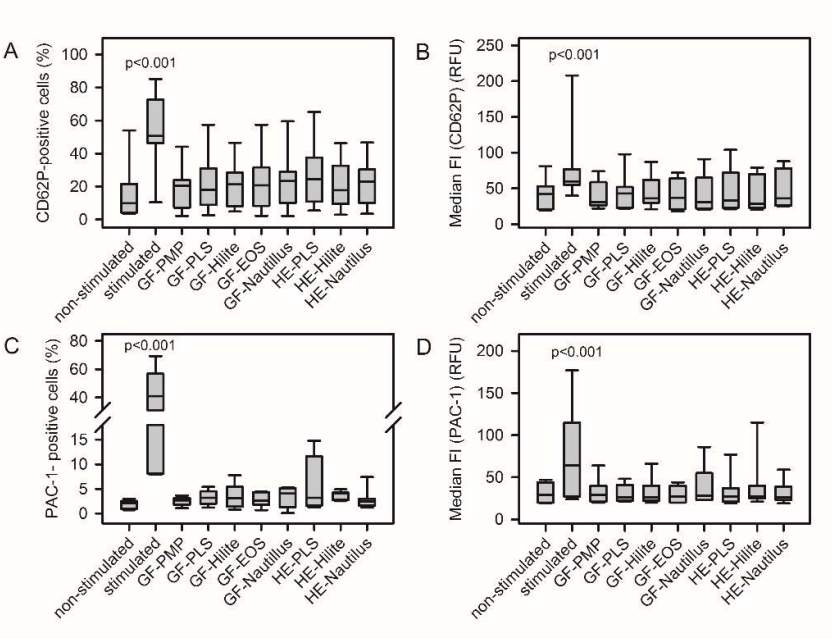

Figure 1. Contact of platelets with ECMO material did not activate platelets regarding the expression of CD62P (A, B) and PAC-1 (C, D). The median fluorescence intensity (median FI) of CD62P-positive and PAC-1-positive cells remained unchanged compared to non-stimulated cells (B, D). Stimulated (non-stimulated) cells were treated with ADP (buffer) without material contact. Stimulated cells presented significantly elevated values of all parameters compared to non-stimulated cells and cells after contact with membrane lung material (GF, gas fibers; HE, heat exchange) from different ($p<0.001$). The different membrane lungs (PLS, Hilite, EOS, Nautilus) represent different antithrombogenic surface coatings (see Table S1). RFU, relative fluorescence intensity.

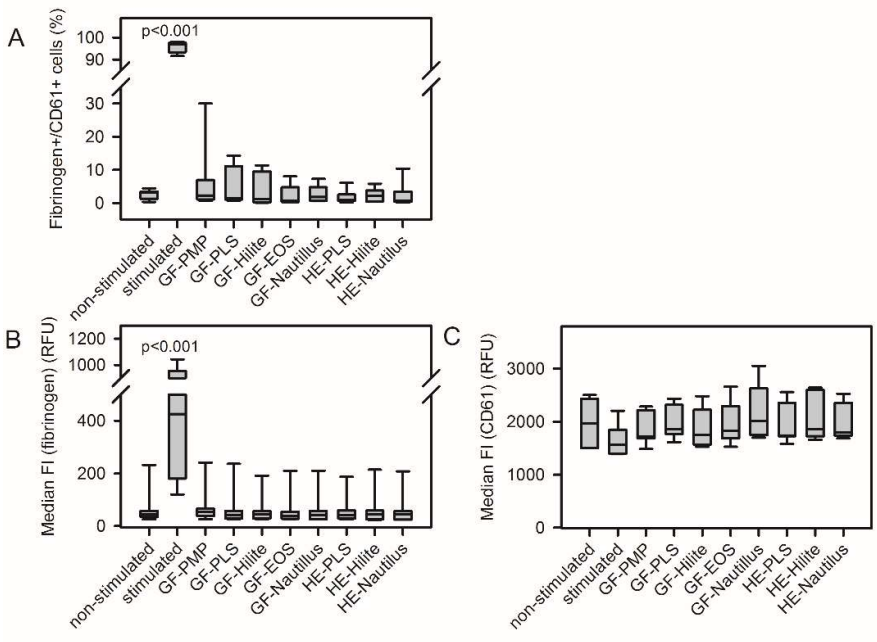

Figure 2. Contact of platelets with ECMO material did not activate platelets regarding the binding of fibrinogen-AlexaFluor488 to CD61-positive platelets. Frequency of double-stained cells (Fibrinogen+/CD61+) (A). Median fluorescence intensity (median FI) of fibrinogen (B) and of CD61 (C) of double stained cells. Stimulated (non-stimulated) cells were treated with ADP (buffer) without material contact. Stimulated cells presented significantly elevated values of the frequency of

 doi:10.20944/preprints202412.0615.v1

fibrinogen+/CD61+ cells and the median FI of fibrinogen compared to non-stimulated cells and cells after contact with membrane lung material (GF, gas fibers; HE, heat exchange) from different ($p<0.001$). The different membrane lungs (PLS, Hilite, EOS, Nautilus) represent different antithrombogenic surface coatings (see Table S1). RFU, relative fluorescence intensity.

3.3. Platelet Adhesion Depended on the ECMO Material

Rhodamine-phalloidin stained F-actin of adherent platelets. As shown in Figure 3, GF-PMP and GF-Hilite presented highest surface coverage with platelets [12 (7-19)% and 13 ((8-19)%, $p=0.330$]. Furthermore, platelet adherence on GF-PMP was significantly higher compared to all other ECMO materials (except GF-Hilite) ($p<0.001$). In addition, platelet adherence on GF-Hilite was signifcantly higher compared to all other ECMO materials (except GF-PMP) ($p<0.001$). Adherence on HE-Hilite was significantly higher compared to HE-PLS ($p=0.029$).

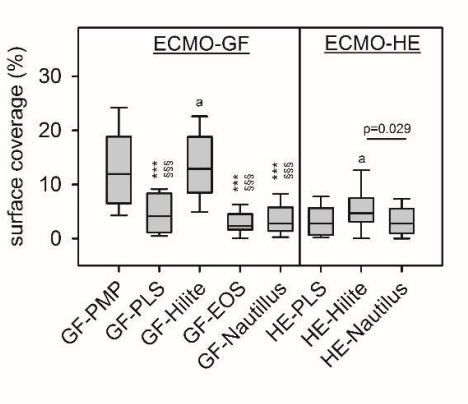

Figure 3. Surface coverage of adherent platelets was significantly higher on GF-PMP and GF-Hilite compared to the other ECMO materials. GF, gas fiber; HE, heat exchanger from different ECMO membrane lungs (MLs). Aderent platelets were stained with rhodamine phalloidin and fluorescence intensity of defined regions of interests on the material surface was determined in 5 different positions on the individual material (see material and methods). Each material was incubated with platelets from 5 different blood donors. GF-PMP was uncoated, while all other GFs and HEs were coated with manufacturer-specific antithrombogenic coatings (see Table S1). Statistics: Two-way ANOVA; $p<0.001$; pairwise comparison using Bonferroni t-test (***; $p<0.001$ compared to GF-PMP; §§§; $p<0.001$ compared to GF-Hilite. Pairwise comparison of HE materials were indicated. a; $p<0.001$ compared GF and HE from Hilite MLs.

Particle sizes of 10-100 µm² were predominant (independent of the test material), while smallest particles (<10 µm²) accounted for only 10-20% of the total particle number (Figure 4). The size distribution on the HEs was different, with significantly more large particles on the HE-Hilite compared to HE-Nautilus and vice versa for the smallest particles. HE-PLS and HE-Hilite were comparable. Furthermore, the size distribution on HE and GF within the Nautilus ML was significantly different (less large particles on the HE, Figure 4C).

 doi:10.20944/preprints202412.0615.v1

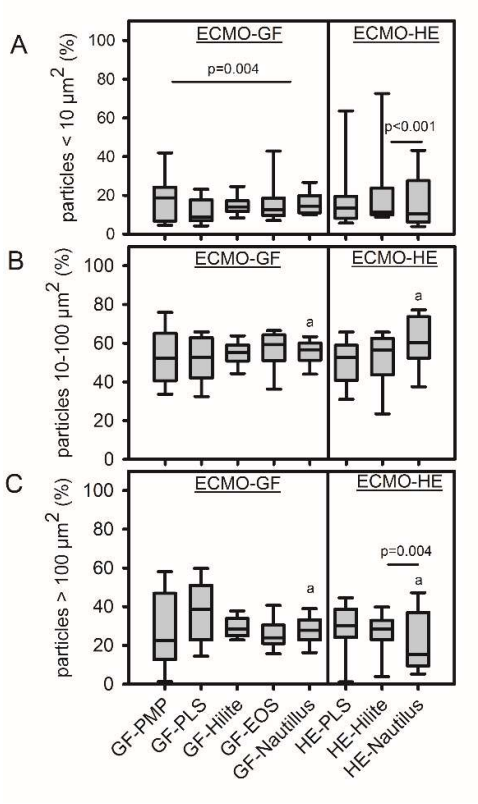

Figure 4. Adherent platelets differed in paticle size. Platelets were subdivided into particle areas of <10 µm² (A); 10-100 µm² (B) and >100 µm² (C). The distribution of the subpopulations was independent of the underlying material surface. GF, gas fiber; HE, heat exchanger from different ECMO membrane lungs (MLs). Experimental setup see Figure 3. Statistics: Two-way ANOVA within ECMO-GFs and ECMO-HEs (A-C); statistical differences were determined for ECMO-GF (A) and ECMO-HEs (A,C) - pairwise comparison using Bonferroni t-test was indicated. a; p=0.005 compared GF and HE from the Nautilus MLs.

4. Discussion

This study used standard laboratory techniques to verify hemocompatibility and thrombogenicity of different artificial surfaces from commercially available new ECMO MLs. While none of the analyzed ECMO materials showed an effect on hemolysis and on platelet activation, the surface of uncoated gas fibers made of PMP (GF-PMP) and the gas fibers from the Hilite-MLs (GF-Hilite) presented significantly higher surface accumulations of platelets compared to the other ECMO materials. The distribution of the cells was even with predominantly medium cell aggregations (10-100 µm²).

Hemolysis is one of the most critical blood reactions of blood contact with artificial surfaces from circulatory assist devices [15]. Under static culture conditions, the direct contact of blood with the material – here, GF and HE with different antithrombogenic surface coatings – did not result in a rupture of RBCs and subsequent release of hemoglobin. The mean hemolysis rate was below 5%. This was in agreement with ISO 10993-4:2017 and ASTM F756-00(2000) and the ECMO materials were therefore classified as non-hemolytic [13,14]. We speculated that hemolysis measured during ECMO therapy (0 – 41%) [15] was not a result of blood contact with artificial surfaces from the ML but a result of shear forces caused from blood pumps or MLs or from patient disease [16-20]. In many clinical studies, elevated levels of plasma free hemoglobin were associated with the development of a pump head thrombosis [4,18,21].

The analysis of platelet activation is an important part of hemocompatibility tests. Platelet activation through biomaterials occurs via adhesion to adsorbed proteins and indirectly through

 doi:10.20944/preprints202412.0615.v1

biomaterial-induced activation of coagulation and other systems [10]. Beside platelet adhesion onto the biomaterial surface (see below), circulating platelets also come into contact with the biomaterial and remained in the soluble phase. Under in vivo conditions, these cells circulate in the blood stream and can induce inflammatory as well as coagulation responses otherwise in the body. In the present study, a simple and rapid static blood incubation model was used [22]. ECMO materials were incubated with PRP without flow conditions and platelet activation of the circulating cells was quantified using FACS analysis (expression of membrane-bond P-selectin, GPIIb/IIIa, GPIIIa and fibrinogen binding) [23]. It was shown, that material contact with platelets did not result in an upregulation of membran receptors and the platelets showed unchanged fibrinogen binding activity. Therefore, we assumed that neither the artificial material (PMP, polyurethane, polyethyleneterephthalate) nor the antithrombotic surface coatings of the different MLs induced platelet activation. However, the used static model did not allow statements about the effect of shear stress on platelet activation during ECMO therapy [3]. Both receptors were found in thrombotic deposits on gas exchange fibers from used MLs and platelet-leukocyte-aggregates (PLAs) were also detected on the surface of the GFs far away from thrombotic aggregates [24,25]. High expression of CD62P on the platelet surface as well as high levels of PLAs were also found in blood samples from ECMO patients [26]. The underlying mechanism remained unclear.

Platelet adhesion is essential to verify the hemocompatibility of a biomaterial [9,10]. In the present study, the cytoskeleton of adherent platelets was stained with rhodamine-phalloidin to evaluate surface coverage of different ECMO materials. This staining strategy revealed the presence of focal adhesion and organized intracellular actin network, supporting the existence of an adhesion process [27]. This is a simple method to visualize platelets and allowed semi-automated quantification. After adherence and fixation, cells were only stained with the fluorescent dye without more processing procedures that ensured realistic cell adhesion. All GFs were made of PMP, they only differed in antithrombogenic surface coatings. Highest surface coverage (10-25%) with platelets was shown for the uncoated GF-PMP as well as the GF-Hilite. While surface coatings with Bioline (PLS), Balance (Nautilus) and PH.I.S.I.O (EOS) prevented extended platelet adhesion compared to the uncoated GF, the X.ELLENCE coating of the Hilite ML remained high. Both, the X.ELLENCE and the Bioline coatings based on heparin and albumin adsorption. Due to manufacturer confidentiality, nothing can be said about the underlying surface chemistry, so this difference cannot be clarified. The same tendency of increased platelet adhesion was also shown for the HE-Hilite with the X.ELLENCE coating. However, HEs were made of different materials (PLS, polyurethane; Hilite and Nautilus, polyethylene terephthalate). Platelets adhered onto the GF and HE in form of microaggregates (10-100 μm^2), while single cells as well as larger aggregates were less prominent. A disadvantage of this detection method is the lack of information about the shape of adherent platelets. Scanning electron microscopy (SEM) as well as immunofluorescence techniques allowed a characterization of the morphology of adhered platelets to verify platelet activation (1, round or discoid, no pseudopodia present; 2, dendritic, early pseudopodial, no flattening; 3, spread dendritic, more pseudopodia flattened, partial hyaloplasm between pseudopodia; 4, fully spread, hyaloplasm fully spread, no distinct pseudopodia, formation of collagen networks) [28,29]. However, SEM is time consuming, expensive and required a special equipment. Therefore, respective analysis failed in the present study. The surface coverage with platelets was less than 10%. Nevertheless, this is a material-induced cell adhesion and demonstrated a risk for restricted hemocompatibility. In the clinical situation, platelet count decreased after ECMO implantation and it was speculated, that the majority of the cells adhered onto the large PMP surfaces of the MLs [4,24]. The results of the present study supported this hypothesis. High shear forces during ECMO therapy due to the blood pump could further enhance this effect. As a result, platelet density and high expression of CD62P was found in thrombotic deposits on the surface of GF from used MLs as well as on the clot-free areas in form of PLAs (platelet-leukocyte aggregates) [24,25].

Limitations: This is an in vitro study to prove the hemocompatibility of clinically already used PMP gas fibers within commercially available new MLs. The used static adhesions model excluded

 doi:10.20944/preprints202412.0615.v1

the effect of shear-forces. However, the significant differences in platelet adhesion based on independent experiments of incubation of all ECMO materials with platelets from 5 different donors.

5. Conclusions

In vitro testing of platelet adhesion disclosed significant differences of ECMO materials with and without different antithrombogenic surface coatings. Instead, circulating platelets remained non-activated. ECMO materials and its coatings were non-hemolytic. Finally, this study confirmed the good hemocompatibility of GFs and HEs from MLs of commercial ECMO systems.

Supplementary Materials: The following supporting information can be downloaded at the website of this paper posted on Preprints.org. Figure S1: Quantification of platelet density on the surface of gas fibers using ImageJ software; Figure S2: Representative flow cytometric analysis of material-induced expression of platelet activation markers; Figure S3: Representative FACS analysis of material-induced fibrinogen binding activity of platelets. Table S1: Coatings and material of commercially available membrane lungs (MLs).

Author Contributions: Conceptualization, K.L. and M.L.; methodology, E.H. and C.T..; software, C.T.; validation, E.H. and C.T..; formal analysis, C.T.; investigation, E.H. and C.T.; resources, K.L.; data curation, C.T. and K.L.; writing—original draft preparation, C.T. and K.L.; writing—review and editing, L.K.; M.L. and K.L.; visualization, K.L.; C.T. and M.L.; supervision, K.L.; project administration, K.L.; funding acquisition, K.L., L.K. All authors have read and agreed to the published version of the manuscript.

Funding: This research was funded by the German Research Foundation (DFG) as part of the Priority Programme (Toward an Implantable Lung) (SPP 2014), grant number 447721607.

Institutional Review Board Statement: The study was conducted in accordance with the Declaration of Helsinki, and approved by the Ethics Committee of the University of Regensburg (protocol code 16-101-0322 and date of approval 2016-11-22).

Informed Consent Statement: Informed consent was obtained from all subjects involved in the study.

Data Availability Statement: Respective data are included in the article/Supplementary Material, and further inquiries from this study can be directed to the corresponding author.

Acknowledgments: The authors thank the staff of the laboratory (Karin Hollnberger, Christina Malterer) for their excellent technical assistance.

Conflicts of Interest: The authors declare no conflicts of interest. The funders had no role in the design of the study; in the collection, analyses, or interpretation of data; in the writing of the manuscript; or in the decision to publish the results.

References

1. Paolone, S. Extracorporeal Membrane Oxygenation (ECMO) for Lung Injury in Severe Acute Respiratory Distress Syndrome (ARDS): Review of the Literature. *Clin. Nurs. Res.* **2017**, *26*, 747-762. doi: 10.1177/1054773816677808.
2. Murphy, D.A.; Hockings, L.E.; Andrews, R.K.; Aubron, C.; Gardiner, E.E.; Pellegrino, V.A., Davis, A.K.. Extracorporeal membrane oxygenation-hemostatic complications. *Transfus. Med. Rev.* **2015**, *29*, 90-101. doi: 10.1016/j.tmrv.2014.12.001.
3. Wang, S.; Griffith, B.P.; Wu, Z.J. Device-Induced Hemostatic Disorders in Mechanically Assisted Circulation. *Clin. Appl. Thromb. Hemost.* **2021**, *27*, 1076029620982374. doi: 10.1177/1076029620982374.
4. Lubnow, M.; Philipp, A.; Foltan, M.; Bull Enger, T.; Lunz, D.; Bein, T.; Haneya, A.; Schmid, C.; Riegger, G.; Müller, T.; et al. Technical complications during veno-venous extracorporeal membrane oxygenation and their relevance predicting a system-exchange--retrospective analysis of 265 cases. *PLoS One.* **2014**, *9*, e112316. doi: 10.1371/journal.pone.0112316.
5. Lehle, K.; Philipp, A.; Foltan, M.; Schettler, F.; Ritzka, M.; Müller, T.; Lubnow, M. Coagulation abnormalities in patients with COVID-19 on venovenous ECLS increased risk for technical complications and support times but had no impact on survival. *Artif. Organs* **2022**, *46*, 1669-1681. doi: 10.1111/aor.14218.
6. Zimmermann, A.K.; Weber, N.; Aebert, H.; Ziemer, G.; Wendel, H.P. Effect of biopassive and bioactive surface-coatings on the hemocompatibility of membrane oxygenators. *J. Biomed. Mater. Res. B Appl. Biomater.* **2007**, *80*, 433–439.
7. Preston, T.J.; Ratliff, T.M.; Gomez, D.; Olshove, V.E. Jr; Nicol, K.K.; Sargel, C.L.; Chicoine, L.G. Modified surface coatings and their effect on drug adsorption within the extracorporeal life support circuit. *J. Extra. Corpor. Technol.* **2010**, *42*, 199–202.

8. Zhang, M.; Pauls, J.P.; Bartnikowski, N.; Haymet, A.B.; Chan, C.H.H.; Suen, J.Y.; Schneider, B.; Ki, K.K.; Whittaker, A.K.; Dargusch, M.S.; Fraser, J.F. Anti-thrombogenic Surface Coatings for Extracorporeal Membrane Oxygenation: A Narrative Review. *ACS Biomater. Sci. Eng.* **2021**, *7*, 4402-4419. doi: 10.1021/acsbiomaterials.1c00758.
9. Gorbet, M.B., Sefton, M.V. Biomaterial-associated thrombosis: roles of coagulation factors, complement, platelets and leukocytes. *Biomaterials* **2004**, *25*, 5681-703. doi: 10.1016/j.biomaterials.2004.01.023.
10. Gorbet, M.; Sperling, C.; Maitz, M.F.; Siedlecki, C.A.; Werner, C.; Sefton, M.V. The blood compatibility challenge. Part 3: Material associated activation of blood cascades and cells. *Acta Biomater.* **2019**, *94*, 25-32. doi: 10.1016/j.actbio.2019.06.020.
11. Amarnath, L.P.; Srinivas, A.; Ramamurthi, A. In vitro hemocompatibility testing of UV-modified hyaluronan hydrogels. *Biomaterials* **2006**, *27*, 1416-24. doi: 10.1016/j.biomaterials.2005.08.008.
12. Horakova, J.; Mikes, P.; Saman, A.; Svarcova, T.; Jencova, V.; Suchy, T.; Heczkova, B.; Jakubkova, S.; Jirousova, J.; Prochazkova, R. Comprehensive assessment of electrospun scaffolds hemocompatibility. *Mater. Sci. Eng. C Mater. Biol. Appl.* **2018,** *82*, 330-335. doi: 10.1016/j.msec.2017.05.011.
13. ISO 10993-4:2017 Biological evaluation of medical devices Part 4: Selection of tests for interactions with blood. Edition 3; **2017**.
14. ASTM F756-13; Standard practice for assessment of hemolytic properties of materials; **2000**.
15. Materne; L.A.; Hunsicker; O.; Menk; M.; Graw; J.A. Hemolysis in patients with Extracorporeal Membrane Oxygenation therapy for severe Acute Respiratory Distress Syndrome - a systematic review of the literature. *Int. J. Med. Sci.* **2021**, *18*, 1730-1738. doi: 10.7150/ijms.50217.
16. Kawahito; S.; Maeda; T.; Motomura; T.; Ishitoya; H.; Takano; T.; Nonaka; K.; Linneweber; J.; Ichikawa; S.; Kawamura; M.; Hanazaki; K.; et al. Hemolytic characteristics of oxygenators during clinical extracorporeal membrane oxygenation. *ASAIO J.* **2002**, *48*, 636-639. doi: 10.1097/00002480-200211000-00010.
17. De Somer; F. Does contemporary oxygenator design influence haemolysis? *Perfusion* **2013**, *28*, 280-285. doi: 10.1177/0267659113483803.
18. Schöps; M.; Groß-Hardt; S.H.; Schmitz-Rode; T.; Steinseifer; U.; Brodie; D.; Clauser; J.C.; Karagiannidis; C. Hemolysis at low blood flow rates: in-vitro and in-silico evaluation of a centrifugal blood pump. *J. Transl. Med.* **2021**, *19*, 2. doi: 10.1186/s12967-020-02599-z.
19. Adamzik; M.; Hamburger; T.; Petrat; F.; Peters; J.; de Groot; H.; Hartmann; M. Free hemoglobin concentration in severe sepsis: methods of measurement and prediction of outcome. *Crit. Care* **2012**, *16*, R125. doi: 10.1186/cc11425.
20. Shaver; C.M.; Upchurch; C.P.; Janz; D.R.; Grove; B.S.; Putz; N.D.; Wickersham; N.E.; Dikalov; S.I.; Ware; L.B.; Bastarache; J.A. Cell-free hemoglobin: a novel mediator of acute lung injury. *Am. J. Physiol. Lung Cell Mol. Physiol.* **2016**, *310*, L532-541. doi: 10.1152/ajplung.00155.2015.
21. Appelt; H.; Philipp; A.; Mueller; T.; Foltan; M.; Lubnow; M.; Lunz; D.; Zeman; F.; Lehle; K. Factors associated with hemolysis during extracorporeal membrane oxygenation (ECMO)-Comparison of VA-versus VV ECMO. *PLoS One.* **2020**, *15*, e0227793. doi: 10.1371/journal.pone.0227793.
22. Weber; M.; Steinle; H.; Golombek; S.; Hann; L.; Schlensak; C.; Wendel; H.P.; Avci-Adali; M. Blood-Contacting Biomaterials: In Vitro Evaluation of the Hemocompatibility. *Front. Bioeng. Biotechnol.* **2018**, *6*, 99. doi: 10.3389/fbioe.2018.00099.
23. Mohan; C.C.; Chennazhi; K.P.; Menon; D. In vitro hemocompatibility and vascular endothelial cell functionality on titania nanostructures under static and dynamic conditions for improved coronary stenting applications. *Acta Biomater.* **2013**, *9*, 9568–9577. doi: 10.1016/j.actbio.2013.08.023.
24. Steiger; T.; Foltan; M.; Philipp; A.; Mueller; T.; Gruber; M.; Bredthauer; A.; Krenkel; L.; Birkenmaier; C.; Lehle; K. Accumulations of von Willebrand factor within ECMO oxygenators: Potential indicator of coagulation abnormalities in critically ill patients? *Artif. Organs* **2019**, *43*, 1065-1076. doi: 10.1111/aor.13513.
25. Wagner; M.S.; Kranz; M.; Krenkel; L.; Pointner; D.; Foltan; M.; Lubnow; M.; Lehle; K. Computer based visualization of clot structures in extracorporeal membrane oxygenation and histological clot investigations for understanding thrombosis in membrane lungs. *Front. Med. (Lausanne)* **2024**, *11*, 1416319. doi: 10.3389/fmed.2024.1416319.
26. Siegel; P.M.; Chalupsky; J.; Olivier; C.B.; Bojti; I.; Pooth; J.S.; Trummer; G.; Bode; C.; Diehl; P. Early platelet dysfunction in patients receiving extracorporeal membrane oxygenation is associated with mortality. *J. Thromb. Thrombolysis* **2022**, *53*, 712-721. doi: 10.1007/s11239-021-02562-9.
27. Picone; P.; Sabatino; M.A.; Ajovalasit; A.; Giacomazza; D.; Dispenza; C.; Di Carlo; M. Biocompatibility; hemocompatibility and antimicrobial properties of xyloglucan-based hydrogel film for wound healing application. *Int. J. Biol. Macromol.* **2019**, *121*, 784-795. doi: 10.1016/j.ijbiomac.2018.10.078.
28. Frank; R.D.; Dresbach; H.; Thelen; H.; Sieberth; H.G. Glutardialdehyde induced fluorescence technique (GIFT): a new method for the imaging of platelet adhesion on biomaterials. *Biomed. Mater. Res.* **2000**, *52*, 374-381. doi: 10.1002/1097-4636(200011)52:2<374::aid-jbm18>3.0.co;2-z.

 doi:10.20944/preprints202412.0615.v1

29. Lehle; K.; Li; J.; Zimmermann; H.; Hartmann; B.; Wehner; D.; Schmid; T.; Schmid; C. In vitro Endothelialization and Platelet Adhesion on Titaniferous Upgraded Polyether and Polycarbonate Polyurethanes. *Materials (Basel)* **2014**, *7*, 623-636. doi: 10.3390/ma7020623.